Food Chemistry 446 (2024) 138898

Contents lists available at ScienceDirect

Food Chemistry

journal homepage: www.elsevier.com/locate/foodchem

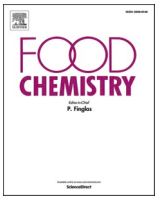

Exploring the formation of heterodimers of barley hydroxycinnamoylagmatines by oxidative enzymes

Annemiek van Zadelhoff, Jean-Paul Vincken, Wouter J.C. de Bruijn *

Laboratory of Food Chemistry, Wageningen University & Research, Bornse Weilanden 9, 6708 WG Wageningen, The Netherlands

ARTICLE INFO

Keywords:
Phenolamide
Hordatine
(Neo)lignanamide
Hydroxycinnamic acid amides
LC-MS
Laccase
Horseradish peroxidase

ABSTRACT

Dimers of hydroxycinnamoylagmatines are phenolic compounds found in barley and beer. Although they are bioactive and sensory-active compounds, systematic reports on their structure-property relationships are missing. This is partly due to lack of protocols to obtain a diverse set of hydroxycinnamoylagmatine homo- and heterodimers. To better understand dimer formation in complex systems, combinations of the monomers coumaroylagmatine (CouAgm), feruloylagmatine (FerAgm), and sinapoylagmatine (SinAgm) were incubated with horseradish peroxidase. For all combinations, the main oxidative coupling products were homodimers. Additionally, minor amounts of heterodimers were formed, except for the combination of FerAgm and CouAgm. Oxidative coupling was also performed with laccases from *Agaricus bisporus* and *Trametes versicolor*, resulting in formation of the same coupling products and no formation of CouAgm-FerAgm heterodimers. Our protocol for oxidative coupling combinations of hydroxycinnamoylagmatines yielded a structurally diverse set of coupling products, facilitating production of dimers for future research on their structure-property relationships.

1. Introduction

Hydroxycinnamoylagmatines (HCAgms) are phenolamides commonly reported in barley (*Hordeum vulgare*) and beer (Pihlava, 2014). HCAgms are composed of a hydroxycinnamic acid moiety linked to an agmatine group by an amide bond (Fig. 1A) (Kristensen, Burhenne, & Rasmussen, 2004). HCAgms and in particular their dimeric coupling products are compounds of interest due to their antifungal (Stoessl, 1967; Stoessl & Unwin, 1970) and α_{1A} adrenoceptor binding activity (Wakimoto et al., 2009). Based on the diverse bioactivities reported for other dimeric phenolamides, the bioactivity of HCAgm coupling products could be even broader than what has been reported thus far (van Zadelhoff et al., 2021). Furthermore, it has been found that HCAgm dimers likely contribute to the astringency of a barley rootlet extract (Kageyama, Inui, Fukami, & Komura, 2011; Kageyama, Inui, Nakahara, & Fukami, 2013). Despite this, studies on the effect of non-volatile compounds on the sensory attributes of beer usually focus on hop-derived compounds, primarily hop bitter acids and flavonoids (Heuberger, Broeckling, Lewis, Salazar, Bouckaert, & Prenni, 2012; Lafontaine et al., 2020). Reports on the sensory attributes of barley-derived phenolic compounds are limited, even though a large diversity of HCAgms and dimers thereof have been found in beer (Pihlava, 2014; Pihlava, Kurtelius, & Hurme, 2016). The dimer content in beer was on average reported to be 5.6 mg/L, whereas the highest reported dimer content was 18.7 mg/L, determined as coumaroylagmatine equivalents based on LC-UV response (Pihlava et al., 2016). This is in a similar range as the hop bitter acid concentration in beer (8–41 mg/L) (Oladokun, Tarrega, James, Smart, Hort, & Cook, 2016). Systematic reports on the structure–property relationships of bioactive and sensory-active HCAgm dimers are missing, in part due to lack of protocols to obtain a diverse set of these molecules. Purification from complex samples such as barley and beer is difficult, labour intense, and costly. Therefore, a better understanding of HCAgm dimer structures, their characterisation in complex mixtures, and the oxidative coupling reactions underlying their formation, is essential to develop protocols for their biomimetic production.

In the plant, exposure to stress induces oxidative coupling of HCAgms into their corresponding dimers (Gorzolka, Bednarz, & Niehaus, 2014; Mikkelsen, Olsen, & Lyngkjær, 2015; Ube, Nishizaka, Ichiyanagi, Ueno, Taketa, & Ishihara, 2017), which belong to the larger class of (neo)lignanamides. Lignanamides are formed by linkages in which both *C*8-carbons are involved and neolignanamides are coupling products in which at least one non-*C*8-carbon is involved (Leonard, Zhang, Ying, & Fang, 2020). The dimeric coupling products in barley,

* Corresponding author.
E-mail addresses: annemiek.vanzadelhoff@wur.nl (A. van Zadelhoff), jean-paul.vincken@wur.nl (J.-P. Vincken), wouter.debruijn@wur.nl (W.J.C. de Bruijn).

https://doi.org/10.1016/j.foodchem.2024.138898
Received 22 December 2023; Received in revised form 16 February 2024; Accepted 27 February 2024
Available online 29 February 2024

known as hordatines, are neolignanamides with an 4-*O*-7′/3-8′-linkage (Fig. 1B). The three most abundant hordatines are the homodimers of coumaroylagmatine (CouAgm) and feruloylagmatine (FerAgm), and the heterodimer of these two monomers (Stoessl, 1967; Stoessl & Unwin, 1970). This heterodimer, commonly referred to as hordatine B, could either be FerAgm-4-*O*-7′/3-8′-DCouAgm or CouAgm-4-*O*-7′/3-8′-DFerAgm. Hordatine B is most commonly depicted as FerAgm-4-*O*-7′/3-8′-DCouAgm (Fig. 1B). However, in most cases no distinction is made between the two aforementioned compounds and it is not specified which of the two is detected, as their differentiation is analytically challenging. A fourth hordatine, a heterodimer of sinapoylagmatine (SinAgm) and FerAgm has also been reported (Gorzolka et al., 2014). Two lignanamides naturally occurring in barley-related *Hordeum* species, *H. murinum* and *H. bulbosium*, are homodimers of FerAgm and are known as murinamides (Ube et al., 2017). Besides variations in the monomeric precursors of the dimers, larger structural diversity of the dimers was reported due to substitutions such as hydroxylation, methylation, and glycosylation (Gorzolka et al., 2014).

In a previous study on the oxidative coupling of hydroxycinnamoylagmatines in single monomer systems with horseradish peroxidase (HRP), the coupling reactivity of the monomers was in line with the order of their peak potentials: sinapoylagmatine (245 mV) > feruloylagmatine (341 mV) > coumaroylagmatine (506 mV). Furthermore, the main coupling products formed upon oxidative coupling of CouAgm and FerAgm by horseradish peroxidase were dimers that naturally occur in barley, namely the 4-*O*-7′/3-8′-linked homodimers. Due to the presence of two methoxy groups on the hydroxycinnamic acid moiety for SinAgm, it cannot form a homodimer with the 4-*O*-7′/3-8′-linkage type, but coupling products with other linkage types can be formed. Upon *in vitro* oxidative coupling of HCAgms with HRP and H_2O_2, dimers linked by five linkage types were identified, namely the 4-*O*-7′/3-8′, 2-7′/8-8′, 8-8′/9-*N*-7′, 8-8′, and 4-*O*-8′ linkages (Fig. 1B) (Van Zadelhoff, Meijvogel, Seelen, de Bruijn, & Vincken, 2022).

Only two types of phenolamides were systematically studied upon enzymatic oxidative coupling: three HCAgms from barley (Van Zadelhoff, Meijvogel, et al., 2022) and one avenanthramide (i.e. hydroxycinnamoylanthranilate) from oat (Okazaki, Ishihara, Nishioka, & Iwamura, 2004; Okazaki, Ishizuka, Ishihara, Nishioka, & Iwamura, 2007). Moreover, these studies did not use mixtures of compounds, as a result of which limited information on the oxidative coupling of phenolamides in combinations is available. The oxidative coupling of hydroxycinnamic acids or monolignols, on the other hand, has been studied much more extensively. The focus of these studies is mainly on the linkage types formed and not on the effect of combining monomers (Magoulas & Papaioannou, 2014). Nonetheless, a few studies report results that could possibly be extrapolated to coupling of phenolamides in mixed systems. Arrieta-Baez *et al.*(Arrieta-Baez & Stark, 2006) described oxidative coupling of four different hydroxycinnamic acids with HRP and H_2O_2 in combinations of two monomers. In all combinations assessed, sinapic acid was always the most reactive monomer. Furthermore, heterodimers were only formed for combinations of caffeic acid with either ferulic acid or sinapic acid (Arrieta-Baez & Stark, 2006). In another study, oxidative coupling of hydroxycinnamic acids in mixtures by either laccase or HRP was tested. When incubating individual compounds, sinapic acid was not always the most reactive. However, when combined with other monomers sinapic acid was consistently the most reactive monomer, followed by ferulic acid (Takahama, 1995). For model systems with mixtures of hydroxycinnamic acids, coumaric acid was the least reactive. Moreover, formation of heterodimers of coumaric acid and ferulic acid has not been reported. Contrary to these observations, homodimers of coumaroylagmatine and heterodimers of coumaroylagmatine and feruloylagmatine are reported as the most abundant dimers in barley (Koistinen et al., 2020). It is therefore interesting to systematically investigate the potential formation of heterodimers upon oxidative coupling for various combinations of phenolamides. Moreover, establishing a protocol for the formation of bioactive and sensory-active HCAgm homo- and heterodimers *in vitro* will be crucial to facilitate production of these compounds for future studies on their structure–property relationships.

As barley contains three different HCAgms, this study will focus on the oxidative coupling of combinations of these HCAgms. The main aims of this study are (i) to understand the formation of HCAgm oxidative coupling products, (ii) to establish a protocol for the *in vitro* production of a diverse set of HCAgm homo- and heterodimers, and (iii) to extrapolate the MS spectral properties obtained for single-monomer systems to a wider range of coupling products, including heterodimers, to aid their identification in complex mixtures. Oxidative coupling in combinations is expected to result in the highest reactivity

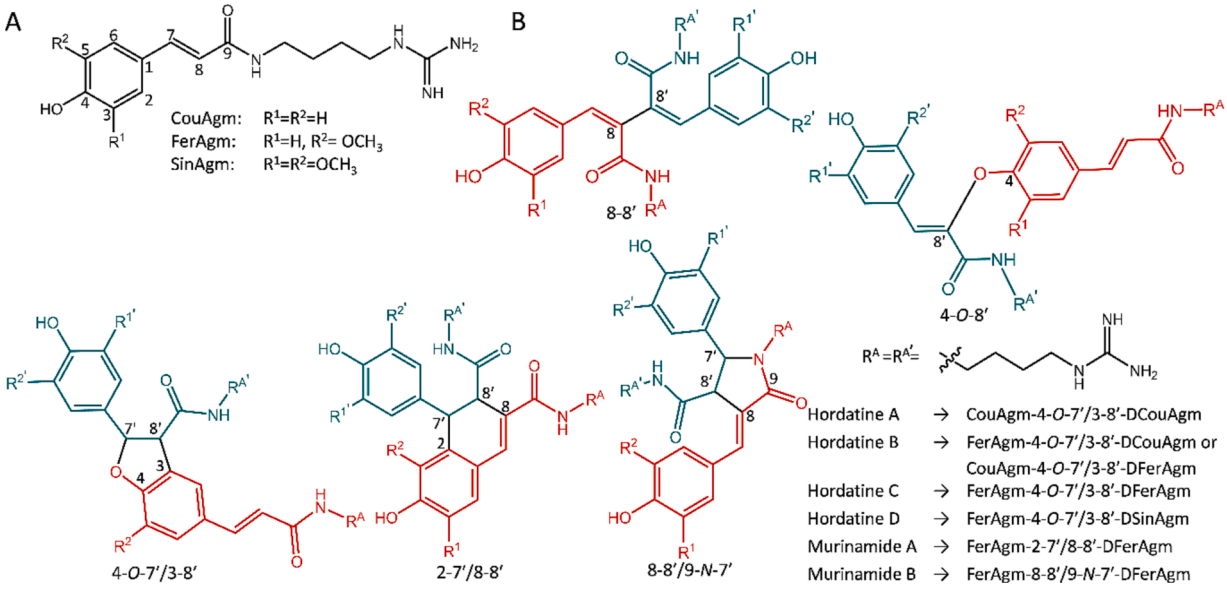

Fig. 1. General structure and abbreviations of hydroxycinnamoylagmatines (HCAgms) (A) and the structure of the previously reported HCAgm dimer linkage types (B), namely, 4-*O*-7′/3-8′, 2-7′/8-8′, 8-8′/9-*N*-7′, 8-8′, and 4-*O*-8′. Naturally occurring dimers and their trivial and systematic names are provided. Monomeric constituents are shown in orange and blue (Kristensen et al., 2004; Stoessl, 1967; Ube et al., 2017; Van Zadelhoff, Meijvogel, et al., 2022). (For interpretation of the references to colour in this figure legend, the reader is referred to the web version of this article.)

for SinAgm, followed by FerAgm, and the lowest reactivity for CouAgm. Furthermore, it is expected that the naturally occurring 4-*O*-7′/3-8′-linkage will be the most abundant linkage type. This will be studied by analysing the monomer conversion and coupling products using reversed-phase ultra-high performance liquid chromatography combined with photodiode array detection and ion trap mass spectrometry (RP-UHPLC-PDA-IT-MS), high-resolution Orbitrap mass spectrometry (RP-UHPLC-PDA-FT-MS), and matrix-assisted laser desorption/ionisation time-of-flight mass spectrometry (MALDI-TOF-MS).

2. Materials and methods

2.1. Materials

p-Coumaric acid (98 %), sinapic acid (98 %), ferulic acid (99 %), *N*,*N*′-dicyclohexylcarbodiimide (DCC), sodium bicarbonate ($NaHCO_3$), sodium hydroxide, 2,2′-azino-bis(3-ethylbenzothiazoline-6-sulfonic acid) (ABTS), nitric acid, horseradish peroxidase type VI-A (HRP, 1.11.1.7, P6782), laccase from *Agaricus bisporus* (1.10.3.2, P40452), laccase from *Trametes versicolor* (1.10.3.2, P38429), deuterated methanol, and 30 % (*w*/*w*) hydrogen peroxide (H_2O_2) were purchased from Sigma-Aldrich (St. Louis, MO, USA). Agmatine sulfate (97 %) was purchased from Fisher Scientific B.V. (Hampton, New Hampshire, USA), and 2,5-dihydroxybenzoic acid was obtained from Bruker Daltonics (Bremen, Germany). Ammonium acetate, potassium dihydrogenphosphate, and dipotassium hydrogen phosphate were purchased from Merck KGaA (Darmstadt, Germany). Glacial acetic acid was purchased from VWR International BV (Radnor, PA, USA). Ethyl acetate, acetone, methanol (MeOH), hexane, HPLC grade acetonitrile (ACN), UHPLC − MS grade ACN and water, and formic acid (FA) (99 % (*v*/*v*)) were purchased from Biosolve (Valkenswaard, Netherlands). Water for purposes other than UHPLC was purified using a Milli-Q purification system equipped with a 0.22 μm filter (Millipore, Molsheim, France).

2.2. Synthesis of hydroxycinnamoylagmatine monomers

p-Coumaroylagmatine (CouAgm), feruloylagmatine (FerAgm), and sinapoylagmatine (SinAgm) were synthesized according to the protocol described by van Zadelhoff *et al.* (van Zadelhoff, Vincken, & de Bruijn, 2022). In short, equimolar amounts of the individual hydroxycinnamic acids and *N*,*N*′-dicyclohexylcarbodiimide (DCC) in acetone were stirred for 1 h at room temperature in the dark. After 1 h, an equimolar amount of agmatine sulfate and sodium bicarbonate dissolved in water was added, in a volume equal to that of the acetone. The mixture was stirred for 24 h at room temperature in the dark, after which the reaction was stopped by adding an equimolar amount of acetic acid. The synthesized HCAgms were purified by flash chromatography using a 12 g FlashPure ID C18 column (Büchi, Flawil, Switserland). The eluents used were water with 1 % (*v*/*v*) FA (eluent A) and ACN with 1 % (*v*/*v*) FA (eluent B). Fractions were collected based on the absorbance at 290, 300, 310, and 320 nm. The elution program used was 2 column volumes (CVs) isocratic at 5 % B, 20 CVs linear gradient to 25 % B, 1 CV linear gradient to 100 % B, and 5 CVs isocratic at 100 % B. After collecting and pooling the fractions containing the desired product, ACN was evaporated under reduced pressure at 40 °C. The remaining water was removed by freeze-drying. Synthesis yield, structural elucidation by NMR, and further characterisation of the synthesised compounds is provided in van Zadelhoff, Vincken, & de Bruijn, 2022.

2.3. Enzymatic oxidative coupling of hydroxycinnamoylagmatines

CouAgm, FerAgm, or SinAgm was separately dissolved in 50 % (*v*/*v*) aqueous ACN to a concentration of 0.05 M. Each monomer solution was mixed with a 0.1 M ammonium acetate buffer at pH 7 in a 1:5 ratio. These solutions were used for single-monomer incubations or were combined in a 1:1 ratio of two or three compounds. To 1.2 mL of the monomer mixtures, 89 μL of enzyme solution was added, either HRP (5 μg/mL), laccase from *Agaricus bisporus* (230 μg/mL), or laccase from *Trametes versicolor* (1.86 mg/mL) was added. The enzyme concentration was based on the enzyme activity as determined using ABTS, and was chosen in such a way that the dosage should theoretically convert all monomers in 120 min. The reactions with both laccases were performed in a thermomixer (Eppendorf, Hamburg, Germany) at 30 °C and 500 rpm. For the reaction with HRP the mixture was equilibrated in a thermomixer (Eppendorf, Hamburg, Germany) at 30 °C and 500 rpm for 5 min. To start the reaction, H_2O_2 (10 μL, 0.3 % (*v*/*v*)) was added. Subsequently, the mixture was incubated in a thermomixer at 30 °C and 500 rpm and samples (10 μL) were taken at 0, 15, 30, 60, and 120 min. The samples were diluted 100 times in water and heated at 90 °C and 500 rpm for 3 min in a thermomixer to inactivate the enzyme. After taking samples at 15, 30, and 60 min, additional H_2O_2 solution (10 μL, 0.3 % (*v*/*v*)) was added to the reaction mixture, which should result in restoring the original H_2O_2 concentration, assuming that all previously added H_2O_2 had reacted. For the combination of CouAgm and FerAgm, three adaptations of the enzymatic oxidative coupling protocol were tested. The first adaptation was an incubation of CouAgm and FerAgm in a 9:1 ratio. The second adaptation was based on gradual addition of FerAgm to the CouAgm reaction. In this experiment, 0.6 mL of CouAgm monomer solution was incubated with a 5 μg/mL HRP solution (89 μL) and the mixture was equilibrated in a thermomixer (Eppendorf, Hamburg, Germany) at 30 °C and 500 rpm for 5 min. To start the reaction, H_2O_2 (10 μL, 0.3 % (*v*/*v*)) was added. After 15, 30, 45, 60, and 75 min 120 μL of the FerAgm solution was added to the reaction. In the third adaptation, the pH was adjusted to 5.3. Besides these adaptations, all other parameters were the same as described for the general protocol. All samples were prepared in triplicate and were analyzed by RP-UHPLC-PDA-IT-MS and RP-UHPLC-PDA-FT-MS. Prior to analysis, the samples were centrifuged (16,000*g*, 5 min).

2.4. Monitoring monomer reactivity and profiling reaction products by RP-UHPLC-PDA-IT-MS analysis

For analysis of HCAgms and their coupling products, the samples were separated on a Thermo Vanquish UHPLC system (Thermo Scientific, San Jose, CA) equipped with a pump, degasser, autosampler, and PDA detector. The flow rate was set at 400 μL/min at a column temperature of 35 °C. The PDA detector was set to measure wavelengths in the range of 190–680 nm. Water (A) and ACN (B), both acidified with 1 % (*v*/*v*) formic acid, were used as eluents. Samples (1 μL) were injected on a Waters Acquity BEH C18 column (150 mm × 2.1 mm i.d., 1.7 μm particle size) with a VanGuard guard column of the same material (5 mm × 2.1 mm i.d., 1.7 μm particle size) (Waters, Milford, MA, USA). The following elution program was used: isocratic at 5 % B for 1.10 min, 1.10–34.02 min linear gradient to 20 % B, 34.02–35.12 min linear gradient to 100 % B, and 35.12–40.61 min isocratic at 100 % B. The eluent was adjusted to its starting composition in 1.10 min followed by equilibration for 5.49 min. Mass spectrometric data were acquired using a Velos Pro linear ion trap mass spectrometer (Thermo Scientific, San Jose, CA, USA) equipped with a heated ESI probe coupled in-line to the Vanquish RP-UHPLC system. Nitrogen was used as sheath gas (50 arbitrary units) and auxiliary gas (13 arbitrary units). The source conditions were a capillary temperature of 263 °C, a probe heater temperature of 425 °C, and a source voltage of 3.5 kV. The S-Lens RF level was 67.63 %. As the HCAgms ionized better in the positive ionization mode, only the positive ionization mode was used. Data was collected in the positive ionization mode over the *m*/*z* range 200–1500. Fragmentation of the most abundant ions in full MS was performed by collision-induced dissociation (CID) with a normalized collision energy of 35 %. Dynamic exclusion with a repeat count of 3, a repeat duration of 5.0 s, and an exclusion duration of 10.0 s was used to obtain MS^2 spectra of multiple different ions present in full MS at the same time. Most settings were optimized via automatic tuning using LTQ Tune Plus (Xcalibur version

4.1, Thermo Scientific). Data processing was performed using Xcalibur 4.1 (Thermo Scientific).

2.5. Accurate mass determination by RP-UHPLC-PDA-FT-MS analysis

To accurately determine the mass of the HCAgms, their coupling products, and the fragments formed, the samples were analysed with RP-UHPLC-PDA and high resolution Orbitrap mass spectrometry (FT-MS). The samples were separated on a Vanquish RP-UHPLC system (Thermo Scientific, San Jose, CA). The injection volume was 1 µL. The column, mobile phases and elution program were identical to those described for RP-UHPLC-PDA-IT-MS analysis.

Accurate mass spectrometric data were acquired using a Thermo Q Exactive Focus hybrid quadrupole-Orbitrap mass spectrometer (Thermo Scientific, San Jose, CA) equipped with a heated ESI probe coupled in-line to the Vanquish RP-UHPLC system. Full MS data were collected over an *m/z* range of 250–800 in PI. Prior to analysis, the mass spectrometer was calibrated in PI using Tune 2.9 software (Thermo Scientific) by injection of Pierce positive ion calibration solution (Thermo Scientific). Nitrogen was used as sheath gas (50 arbitrary units) and auxiliary gas (13 arbitrary units). The source conditions were a capillary temperature of 263 °C, a probe heater temperature of 425 °C and a source voltage of 3.5 kV. The S-Lens RF level was 50 %. Fragmentation was performed by higher-energy collisional dissociation (HCD) with a normalised collision energy of 15 %. Full MS and MS^2 data were recorded at 70,000 and 17,500 resolution, respectively. Data processing was performed using Xcalibur 4.1 (Thermo Scientific).

2.6. Oligomer analysis by MALDI-TOF-MS

The formation of larger oligomers upon enzymatic oxidative coupling (t = 120 min) was investigated using matrix-assisted laser desorption/ionisation time of flight mass spectrometry (MALDI-TOF-MS). Untreated monomer solutions (t = 0) were also analysed to verify the absence of larger coupling products prior to enzymatic treatment (data not shown). 2,5-Dihydroxybenzoic acid was used as a matrix. Spots were prepared by mixing 1 µL of the matrix solution with 1 µL of the sample on a MTP 384 ground steel target plate (Bruker Daltonics). Mass spectra (*m/z* 260–3000 for the untreated solutions and *m/z* 500–3000 for the treated solutions) were obtained in the positive ionization mode using an Autoflex maX workstation equipped with a Smartbeam-II laser of 355 nm controlled by FlexControl 3.4 software (Bruker Daltonics). Spectra were collected at a laser intensity of 35 % with an ion source voltage of 18.90 kV. The frequency of the laser was 500 Hz. The system was calibrated using maltodextrin. All samples were analysed in duplicate. Data processing was performed using FlexAnalysis 3.4 (Bruker Daltonics).

3. Results and discussion

3.1. Reactivity upon enzymatic oxidative coupling by HRP

In order to better understand oxidative coupling of hydroxycinnamoylagmatines (HCAgms), which is part of the plants' stress response in *Hordeum* species, the *in vitro* oxidative coupling of these compounds in mixtures was studied. To this end, combinations of two or three HCAgm monomers were incubated with horseradish peroxidase (HRP) for two hours. The conversion of the monomers was determined based on the relative MS peak area observed in RP-UHPLC-PDA-IT-MS, as shown in Fig. 2A. In all systems, the order of reactivity, from highest to lowest was: SinAgm > FerAgm > CouAgm. This order of reactivity was the same as was observed in single-monomer systems and follows the order of the peak potentials of the monomers, being 245 mV for SinAgm, 341 mV for FerAgm, and 506 mV or CouAgm (Van Zadelhoff, Meijvogel, et al., 2022). The peak potential is a measure for the ease of oxidation of a molecule and can, therefore, be used as a measure for the reactivity of the monomers upon incubation with HRP. For all incubations with CouAgm it can be observed that the CouAgm monomer was not involved in the coupling reaction until most of the SinAgm and/or FerAgm had reacted. The observed order of reactivity is also in line with results reported for combinations of hydroxycinnamic acids incubated with HRP (Arrieta-Baez & Stark, 2006). Additionally, the overall

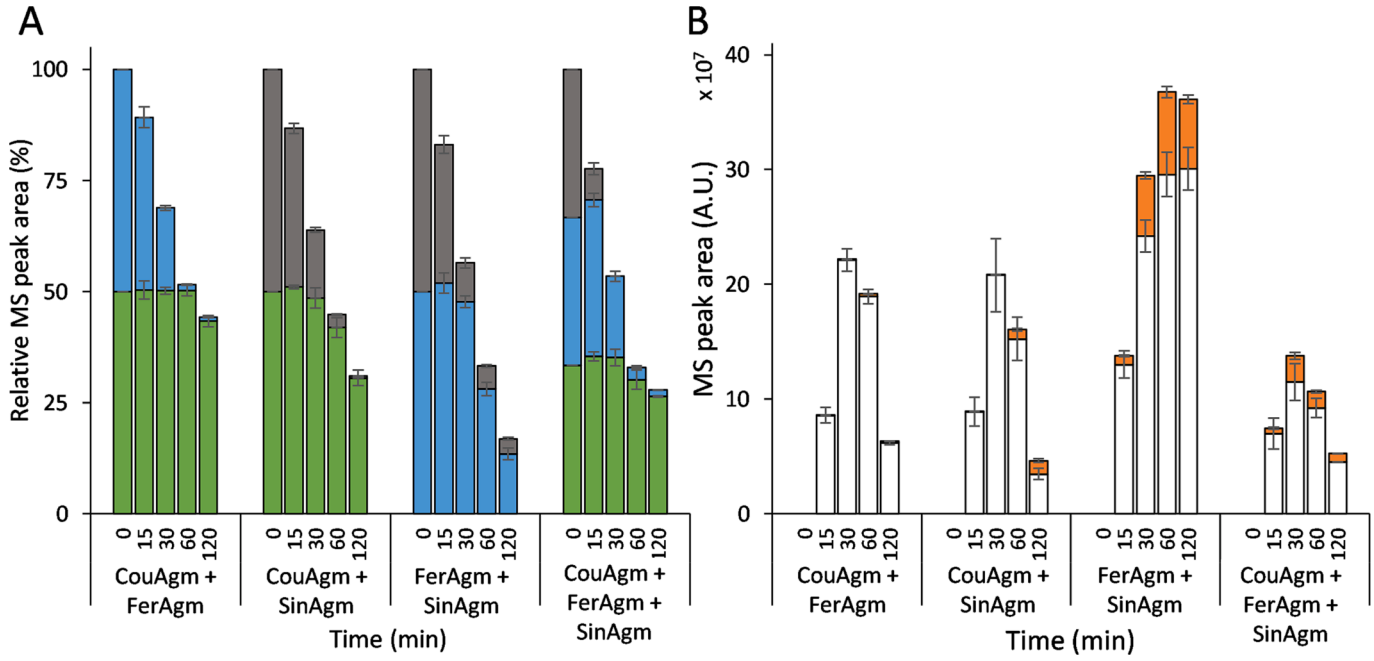

Fig. 2. Percentage of remaining monomer upon oxidative coupling of combinations of coumaroylagmatine (CouAgm, green), feruloylagmatine (FerAgm, blue), and sinapoylagmatine (SinAgm, grey) with horseradish peroxidase and H_2O_2, expressed as the relative MS extracted ion peak area of the corresponding peak in RP-UHPLC-PDA-IT-MS (A). Total MS peak area of the homodimers (white) and heterodimers (orange) formed over time (B). Error bars display the standard deviation based on triplicates. A.U., arbitrary units. (For interpretation of the references to colour in this figure legend, the reader is referred to the web version of this article.)

total monomer conversion was the lowest in systems with CouAgm. We hypothesize that further oxidative coupling of the initial coupling products was preferred over coupling of the remaining CouAgm monomer. To investigate this hypothesis, the total MS peak area of the dimeric coupling products was determined (Fig. 2B), based on tentative identification of the products by previously developed MS methods (Van Zadelhoff, Meijvogel, et al., 2022). In-depth identification of dimeric products will be described in section 3.2. For all incubations with CouAgm, the dimer content increased over time until the time point of 30 min, after which the dimer content decreased. This indicated that FerAgm dimers and SinAgm dimers were more prone to oxidation by HRP compared to the CouAgm monomer, which supports the aforementioned hypothesis. For hydroxycinnamic ethyl esters and their dimeric products the peak potentials of the dimers formed were previously reported (Neudörffer, Bonnefont-Rousselot, Legrand, Fleury, & Largeron, 2004). In that study, the peak potential of the ferulate ethyl ester was set as 0 mV and interestingly, the relative peak potentials of the ferulate ethyl ester dimers were reported to be lower than those of the monomers, namely − 130 mV (8-8′-linked), −150 mV (4-*O*-7′/3-8′-linked), and − 220 mV (2-7′/8-8′-linked) (Neudörffer et al., 2004). The peak potential of the coumarate ethyl ester was 200 mV higher compared to the ferulate ethyl ester, resulting in an even bigger expected gap between the CouAgm monomer and FerAgm dimers. This suggests that the dimers can be more easily oxidised than the monomers, which is in line with our result that the dimer content decreased when monomers were still present, thereby supporting our hypothesis.

3.2. Characterization of homo- and heterodimeric coupling products

The chromatograms obtained after 60 min of incubation of the HCAgm mixtures with HRP and H_2O_2 are shown in (Fig. 3. The obtained product profile was determined by non-targeted and targeted approaches, in which $UV_{320\ nm}$, full MS, and extracted ion chromatograms focussed on the *m/z* of the expected heterodimers and homodimers were used. The full MS and extracted ion chromatograms are provided in Supplementary data (Figure S1 and S2). Based on the RP-UHPLC-MS data, a large variety of coupling products was formed upon enzymatic oxidation by HRP. Homodimers could be identified based on the fragmentation data and retention times of the products that were previously purified and identified by NMR in single-monomer systems (Van Zadelhoff, Meijvogel, et al., 2022). Heterodimer yields were low and retention times of homodimers and heterodimers within each reaction mixture were very close, thereby hindering purification. Thus, we decided to focus on annotation of the reaction products by LC coupled to (high resolution) MS, based on retention times and fragmentation rules that were previously established for homodimers (Van Zadelhoff, Meijvogel, et al., 2022). In this way, the main heterodimeric products could be tentatively identified. The MS^2 spectra of two tentatively identified heterodimers and of one previously identified homodimer are shown in Fig. 4, as an example of how fragmentation patterns were matched. The MS^2 spectra for the other tentatively identified heterodimers and comparison with the identified homodimer with the same linkage type are provided in Supplementary data (Table S1-S4). Using this approach, thirteen compounds were (tentatively) identified.

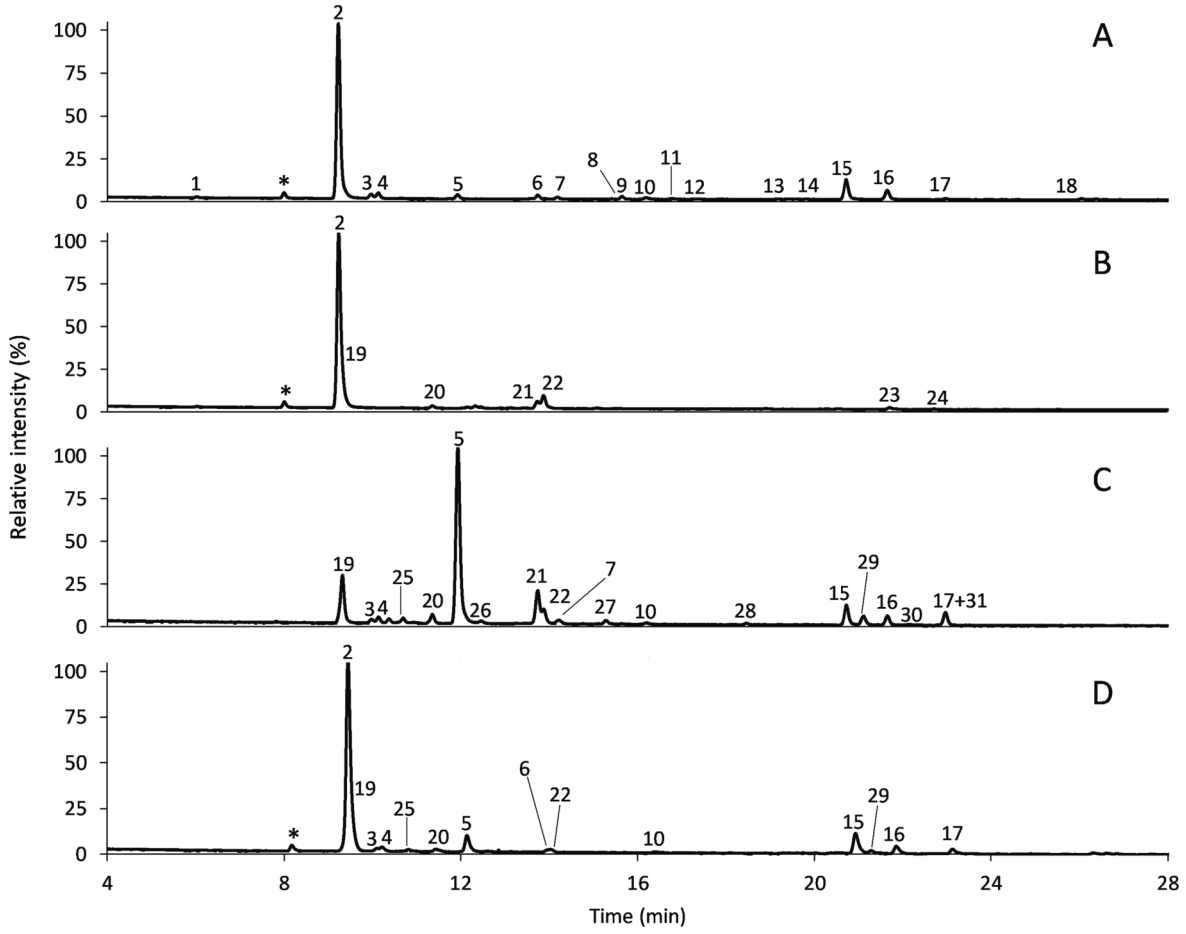

Fig. 3. RP-UHPLC-PDA $UV_{320\ nm}$ chromatograms of CouAgm + FerAgm (A), CouAgm + SinAgm (B), FerAgm + SinAgm (C), and a combination of all three monomers (D) after 60 min of incubation with HRP and H_2O_2. Peak numbers refer to the (tentatively) identified compounds listed in Table 1 and unidentified compounds listed in Supplementary data (Table S5). * indicates an impurity present since the beginning of the reaction, which was not converted during the oxidative coupling reaction. RP-UHPLC-PDA-IT-MS full MS and extracted ion chromatograms are provided in supplementary data (Figure S1 and S2).

Furthermore, seven dimers with six linkage types that could not be determined were detected. These dimers are most likely linked by a linkage type other than the linkage types reported for the identified dimers. An overview of the identified compounds is provided in Table 1, and an overview of the UHPLC-PDA-ESI-IT-MS data for all coupling products is provided in Supplementary data (Table S5). The main products formed upon incubation of combinations of HCAgms with HRP are homodimers (Fig. 2B, Fig. 3). It should be noted that no chiral separation of stereoisomers was performed and that we cannot draw any conclusion on whether the oxidative coupling by HRP is stereospecific. In some model systems, up to four stereoisomers were detected, most likely corresponding to (a combination of) *cis/trans* isomers and/or diastereomers.

3.3. Determining the monomer composition of 4-*O*-7′/3-8′-linked dimers

FerAgm homodimers and CouAgm-SinAgm heterodimers are isomeric structures. Fig. 4 shows the fragmentation patterns of these isomers and two other dimers with the same linkage type for comparison. Spectra 4B and 4C correspond to the structural isomers FerAgm-4-*O*-7′/3-8′-DFerAgm (15, and stereoisomer 16) and CouAgm-4-*O*-7′/3-8′-DSinAgm (23, and stereoisomer 24). These four compounds (15, 16, 23, and 24) form the same main fragments in both MS^2 and MS^3 (MS^2 in Fig. 4 and MS^3 in Supplementary data; Figure S3). Additionally, compound 16 (RT 21.74 min) and compound 23 (RT 21.82 min) practically elute at the same time. In our two-monomers combinations, these isomers could be easily differentiated as they do not coexist in the same sample. For samples in which they could coexist, e.g. barley extracts, it should be considered that differentiating between these dimers is difficult due their similar chromatographic and mass spectrometric behaviour. A more detailed comparison of the fragmentation patterns by IT-MS and identification of fragments by high resolution FT-MS with HCD fragmentation was used to confirm the identity of two diagnostic fragments, namely fragment I^{2+} and J^{+} (Fig. 4). The fragment I^{2+} for FerAgm-4-*O*-7′/3-8′-DFerAgm (*m/z* 230.14520, $C_{22}H_{36}O_3N_8^{2+}$, Δ1.00 ppm) differs by OCH_2, indicating the presence of a methoxy group instead of a hydrogen atom, compared to I^{2+} for CouAgm-4-*O*-7′/3-8′-DSinAgm (*m/z* 215.13950, $C_{21}H_{34}O_2N_8^{2+}$, Δ-0.87 ppm). Similarly, fragment J^{+} for FerAgm-4-*O*-7′/3-8′-DFerAgm (347.17130, $C_{17}H_{23}O_4N_4^{+}$, Δ −0.24 ppm) differs by OCH_2 compared to J^{+} for CouAgm-4-*O*-7′/3-8′-DSinAgm (*m/z* 317.16125, $C_{16}H_{21}O_3N_4^{+}$, Δ 1.37 ppm). The fact that the *m/z* of both of these fragments in CouAgm-4-*O*-7′/3-8′-DSinAgm is lower by a methoxy group thus indicates that the fragment involves the CouAgm moiety. Based on this, the fragment could be identified (Fig. 4). Fragment J^{+} is single charged and based on the elemental composition this fragment differs from fragment I^{2+} by $C_5H_{13}N_4$, corresponding to the additional loss of one of the agmatine moieties. Fragment J^{+} is therefore identified as fragment $I^{2+}-C_5H_{13}N_4$. When comparing the MS^2 spectra for these two compounds to the MS^2 spectra of FerAgm-4-*O*-7′/3-8′-DSinAgm and CouAgm-4-*O*-7′/3-8′-DCouAgm it becomes apparent that these two fragments can be used to determine whether the monomeric precursor presented in orange in Fig. 4 is a CouAgm or FerAgm moiety. These two diagnostic fragments can therefore be used to distinguish between the FerAgm-4-*O*-7′/3-8′-DFerAgm homodimer and the CouAgm-4-*O*-7′/3-8′-DSinAgm heterodimer. It should be noted that these fragments were consistently generated by CID and not always by HCD.

These two diagnostic fragments can aid analysis of HCAgm dimers in more complex samples in which more structural diversity is theoretically possible. Typically only the FerAgm homodimer is reported in literature, however, it is unclear whether the CouAgm and SinAgm heterodimer is absent in barley, or that it is overlooked or wrongly assigned due to the highly similar retention time and mass spectra of these dimers. It is important to consider the similarities between these compounds for future analyses on barley extracts. Furthermore, the diagnostic fragments presented here can aid in distinguishing CouAgm-4-*O*-7′/3-8′-DFerAgm and FerAgm-4-*O*-7′/3-8′-DCouAgm in complex samples, if they are at least partially chromatographically separated. Typically this heterodimer is depicted as FerAgm-4-*O*-7′/3-8′-DCouAgm (Pihlava et al., 2016; Smith & Best, 1978; Stoessl *et al.*, 1970), even though both coupling options are possible. In addition to the presented examples, these diagnostic fragments can be used more generally to determine the monomer composition, and to elucidate which monomer donates the oxygen to the furan in 4-*O*-7′/3-8′-linked phenolamide dimers.

3.4. Driver for heterodimer formation is still unknown

In our systems, four linkage types were found for heterodimers of FerAgm and SinAgm, three of which are shown in Table 1 (compounds 25, 26/27, 29/31) and one of which (compound 30) can be found in the supplementary data (Table S5). For heterodimers of CouAgm and SinAgm (compounds 23/24), only one linkage type was detected. The larger amount of monomer converted for the combination of FerAgm and SinAgm, i.e. 87.4 % after 120 mins (Fig. 2), likely contributes to an overall larger variety of detectable coupling products compared to the other combinations. With regards to the linkage types of FerAgm and SinAgm, the 4-*O*-7′/3-8′-linkage was the only linkage type reported. Based on the fragments observed for one of our products, we tentatively identified 8-8′/9-*N*-7′-linked heterodimers of FerAgm and SinAgm (compounds 26 and 27). It is, however, not possible to determine whether the compound is FerAgm-8-8′/9-*N*-7′-DSinAgm or SinAgm-8-8′/9-*N*-7′-DFerAgm based on the fragmentation pattern.

Due to the presence of two methoxy groups on the benzene ring of SinAgm, SinAgm is unable to form the 4-*O*-7′/3-8′-linkage, which is the most abundant linkage formed for all other incubations. Instead, SinAgm forms the 2-7′/8-8′-linkage as the most abundant linkage type.

The formation of heterodimers was limited in all systems, with at least 75 % of all coupling products being homodimers (Fig. 2B). The largest relative amount of heterodimers formed was observed for the combination of SinAgm and FerAgm and the lowest relative amount of heterodimers was formed for CouAgm and FerAgm.

Similarly, Arrieta-Baez and Stark (2006) reported limited formation of heterodimers for hydroxycinnamic acids upon coupling using HRP and H_2O_2, as no heterodimers were formed in two-compound combinations of sinapic acid, ferulic acid, and coumaric acid. The only combination of hydroxycinnamic acids for which heterodimers were reported are combinations of caffeic acid with either sinapic acid or ferulic acid. This study did not report the percentage of monomer converted during the experiment, so it is not clear whether the conversion potentially limited heterodimer formation (Arrieta-Baez & Stark, 2006). Caffeic acid and sinapic acid have similar peak potentials (183 mv and 188 mV, respectively) and ferulic acid has a higher peak potential (335 mV) (Gaspar et al., 2009). In other studies in which the combination of coumaric acid and ferulic acid was incubated with HRP and H_2O_2, no heterodimers were formed either, similarly to our results (Arrieta-Baez et al., 2012; Baydoun, Pavlencheva, Cumming, Waldron, & Brett, 2004).

According to various other studies, the formation of heterodimers, which is also referred to as cross-coupling, can be affected by radical formation rates and diffusion-controlled processes (Elsler, Wiebe, Schollmeyer, Dyballa, Franke, & Waldvogel, 2015; Leifert & Studer, 2020; Syrjänen & Brunow, 1998). The three most common parameters used to explain or predict cross-coupling are peak potential, reaction rates, and nucleophilicity of compounds (Leifert et al., 2020; Schön, Kaifer, & Himmel, 2019). The first parameter, the effect of the peak potential, differs between studies. It has, for example, been reported that a difference of at least 0.25 V in peak potential is needed for cross-coupling to occur (Kočovský, Vyskočil, & Smrcina, 2003), whereas other studies reported cross-coupling for compounds within a restricted range of peak potentials (Syrjänen & Brunow, 1998). In our combinations, FerAgm and SinAgm have the smallest difference in peak potential (0.10 V) (Van Zadelhoff, Meijvogel, et al., 2022), and CouAgm and

SinAgm have the largest difference in peak potential (0.26 V) (Van Zadelhoff, Meijvogel, et al., 2022). Despite this, cross-coupling occurred in both systems, thus the occurrence or lack of heterodimer formation could not be predicted based on the difference in peak potential. The second parameter, the effect of reaction rates, is linked to a theory in which the formation of heterodimers is linked to significantly different rate constants for self-coupling of the compounds (also called the self-reaction rate), while both compounds form radicals at an equal rate. According to this theory, for species forming a stable radical, resulting in a low self-reaction rate (i.e. a persistent radical), coupling with a more reactive radical species with a similar peak potential (i.e. a transient radical) is more favourable than self-coupling, resulting in cross-coupling. For the transient radical two options are favourable, cross-coupling and self-coupling. This theory is known as the persistent radical effect (PRE) (Leifert & Studer, 2020). In our single-monomer systems, the self-coupling was fastest for SinAgm and due to the differences in peak potentials the radical formation rate will be different (Van Zadelhoff, Meijvogel, et al., 2022). Therefore, SinAgm does not act as the persistent radical and the formation of heterodimers containing SinAgm cannot be explained by the PRE. The third parameter, nucleophilicity, is employed in theories which propose that cross-coupling between two compounds will only occur if the compound with a higher oxidation potential has a lower global nucleophilicity. The nucleophilicity is relative to the energy of the highest occupied molecular orbital (HOMO) of the compounds (Libman, Shalit, Vainer, Narute, Kozuch, & Pappo, 2015). For the corresponding hydroxycinnamyl alcohols, the HOMO energy increases in the order sinapyl alcohol < feruloyl alcohol < coumaryl alcohol (Akman, 2019). The nucleophilicity of our tested compounds is unknown, but is expected to increase in the same order (i.e. SinAgm < FerAgm < CouAgm), which is also the order in which the oxidation potential increases. Therefore, this theory based on nucleophilicity cannot explain the observed cross-coupling. In conclusion, none of the previously proposed theories explain the formation of heterodimers in the investigated systems, but heterodimer formation was observed in our model systems and *in vivo*.

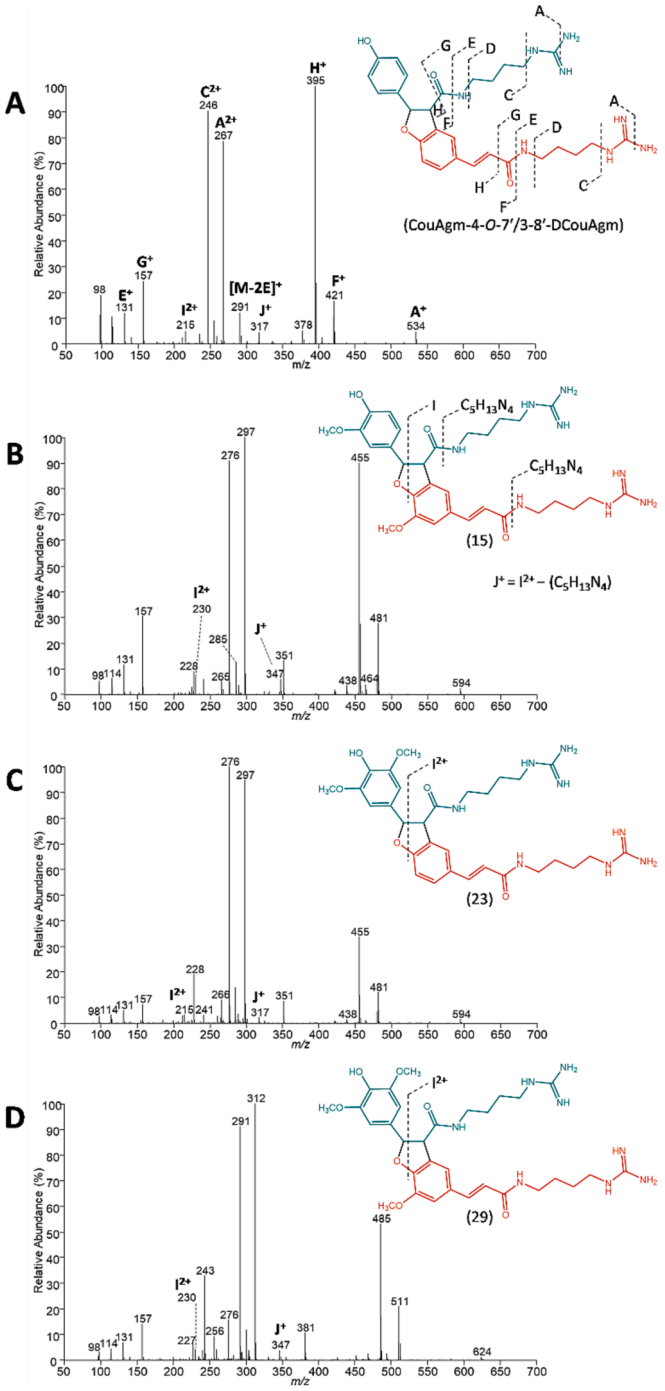

Fig. 4. Examples of ESI-IT-MS^2 CID fragmentation spectra for three dimers linked with the 4-*O*-7′/3-8′-linkage. FerAgm-4-*O*-7′/3-8′-DFerAgm (15, B) was previously identified (Van Zadelhoff, Meijvogel, et al., 2022) and compounds CouAgm-4-*O*-7′/3-8′-DSinAgm (23, C) and FerAgm-4-*O*-7′/3-8′-DSinAgm (29, D) were identified based on matching fragmentation patterns. Diagnostic fragments I and J are indicated. The MS^2 spectrum for CouAgm-4-*O*-7′/3-8′-DCouAgm and typical fragments A-H (A) were reported previously (Van Zadelhoff, Meijvogel, et al., 2022).

3.5. *Formation of FerAgm-4-O-7′/3-8′-DCouAgm is not observed*

Noteworthily, one of the dimers commonly reported in barley, FerAgm-4-*O*-7′/3-8′-DCouAgm (commonly referred to as hordatine B) (Stoessl, 1967; Stoessl *et al.*, 1970), was not formed in any system containing the combination of CouAgm and FerAgm. Since CouAgm-4-*O*-7′/3-8′-DSinAgm was formed from CouAgm and SinAgm (peak potential Δ0.26 V), the relatively large difference in peak potential does not explain why CouAgm and FerAgm (peak potential Δ0.17 V) would not form a heterodimer.

Based on the monomer conversion data presented in Fig. 2A, it can be concluded that no CouAgm was converted as long as FerAgm monomer remained present, whereas some CouAgm was converted in the incubation with SinAgm even before all SinAgm had reacted. To investigate whether the reaction conditions can steer the reaction towards the formation of FerAgm-4-*O*-7′/3-8′-DCouAgm, or other heterodimers of FerAgm and CouAgm, two adjusted protocols were tested. Firstly, an incubation was performed with a 9:1 M ratio of CouAgm to FerAgm. Secondly, an incubation was performed with a 1:1 final molar ratio but in which 0.2 equivalent FerAgm was added gradually after every 15 min, starting after 15 min of pre-incubation of only CouAgm, HRP, and H_2O_2. For these protocols, the concentration of CouAgm was always higher than that of FerAgm, and CouAgm was therefore expected to become partially radicalised by HRP and subsequently available for coupling with FerAgm. Despite this, neither protocol resulted in the formation of FerAgm-4-*O*-7′/3-8′-DCouAgm (data not shown). Thus, relative concentration of the monomers does not affect the formation of this heterodimer. In a previous report on enzymatic formation of heterodimers of FerAgm, the pH affected the linkage type formed (Ube et al., 2017). However, this was not the case for CouAgm at pH 5, 7, and 8 under the same conditions (Van Zadelhoff, Meijvogel, et al., 2022). It was shown that the oxidative enzymes that are likely to be involved with the formation of 4-*O*-7′/3-8′-linked dimers are located in the vacuole (Kristensen, Bloch, & Rasmussen, 1999; Ube, Ishihara, Yabuta, Taketa, Kato, & Nomura, 2023; Zipor & Oren-Shamir, 2013). Based on results for wheat and rice the pH in the vacuole is expected to be around 5.2 or 5.3 (Kulichikhin, Aitio, Chirkova, & Fagerstedt, 2007). We therefore also

Table 1
Spectral data and (tentative) identification of hydroxycinnamoylagmatine oxidative coupling products after 60 min of incubation with HRP and H_2O_2. Only fragments with a relative abundance above 10 % are reported. Peak numbers correspond to numbers in Fig. 3. Trivial names of the dimers, if available, are provided in parentheses.[a]

	UHPLC-PDA-ESI-IT-MS					ESI-FT-MS				
Peak no.	RT (min)	λ_{max} (nm)	Ionization	*m/z*	MS^2 (*m/z*) (relative abundance)	Molecular formula	Observed *m/z*	Theoretical *m/z*	Error (ppm)	(Tentative) identification
1	6.10	n.d.	$[M+H]^+$	277	260 (100), 114 (20), 217 (18), 261 (11)	$C_{14}H_{20}O_2N_4$	277.16602	277.16590	0.42	*cis*-CouAgm [b]
2	9.32	294	$[M+H]^+$	277	260 (100), 114 (15), 217 (15), 115 (11)	$C_{14}H_{20}O_2N_4$	277.16589	277.16590	−0.05	*trans*-CouAgm [b]
3	10.06	350	$[M+2H]^{2+}$	306	241 (100), 131 (97), 227 (73), 464 (72), 481 (62), 297 (49), 285 (47), 276 (41), 114 (36), 422 (29), 157 (28), 323 (27), 594 (24), 436 (22), 482 (22), 298 (20), 465 (17), 340 (16), 439 (11), 421 (10)	$C_{30}H_{42}O_6N_8$	306.16867	306.16864	0.09	FerAgm-8-8′-FerAgm [b]
4	10.20	342	$[M+2H]^{2+}$	306	241 (100), 131 (45), 481 (44), 265 (43), 276 (32), 227 (30), 285 (29), 464 (27), 297 (25), 179 (21), 114 (21), 422 (21), 298 (18), 323 (17), 482 (17), 157 (15), 261 (15), 594 (13), 426 (11), 264 (10)	$C_{30}H_{42}O_6N_8$	306.16873	306.16864	0.29	FerAgm-2-7′/8-8′-DFerAgm [b]
5	12.02	334	$[M+H]^+$	307	290 (100), 177 (21), 291 (15), 114 (14), 247 (13), 248 (11)	$C_{15}H_{22}O_3N_4$	307.17657	307.17647	0.35	*trans*-FerAgm [b]
6	13.84	n.d.	$[M+2H]^{2+}$	306	276 (100), 297 (32), 285 (12)	$C_{30}H_{42}O_6N_8$	306.16870	306.16864	0.19	FerAgm-8-8′/9-*N*-7′-DFerAgm [b]
11	16.87	n.d.	$[M+2H]^{2+}$	306	297 (100), 455 (95), 276 (68), 481 (35), 351 (35), 157 (29), 131 (29), 456 (27), 285 (21), 228 (19), 114 (11), 464 (10), 482 (10)	$C_{30}H_{42}O_6N_8$	306.16867	306.16864	0.09	FerAgm-4-*O*-7′/3-8′-DFerAgm [b,c](hordatine C)
12	17.43	n.d.	$[M+2H]^{2+}$	306	297 (100), 455 (89), 276 (65), 351 (35), 481 (32), 456 (29), 157 (27), 131 (23), 285 (19), 228 (17), 482 (13), 265 (12), 114 (11)	$C_{30}H_{42}O_6N_8$	306.16870	306.16864	0.19	FerAgm-4-*O*-7′/3-8′-DFerAgm [b,c](hordatine C)
15	20.81	326	$[M+2H]^{2+}$	306	297 (100), 455 (89), 276 (84), 157 (27), 456 (24), 481 (21), 285 (13), 351 (10)	$C_{30}H_{42}O_6N_8$	306.16876	306.16864	0.39	FerAgm-4-*O*-7′/3-8′-DFerAgm [b,c](hordatine C)
16	21.74	326	$[M+2H]^{2+}$	306	297 (100), 455 (94), 276 (86), 157 (31), 456 (26), 481 (24), 285 (13), 131 (10), 351 (10)	$C_{30}H_{42}O_6N_8$	306.16873	306.16864	0.29	FerAgm-4-*O*-7′/3-8′-DFerAgm [b,c](hordatine C)
17	23.06	n.d.	$[M+2H]^{2+}$	306	276 (100), 297 (51), 289 (11)	$C_{30}H_{42}O_6N_8$	306.16864	306.16864	−0.01	FerAgm-4-*O*-8′-FerAgm [b]
19	9.41	314	$[M+2H]^{2+}$	336	306 (100), 271 (80), 315 (76), 361 (69), 327 (63), 131 (59), 328 (52), 383 (43), 370 (39), 541 (37), 157 (35), 181 (25), 344 (21), 114 (19), 513 (16), 301 (16), 396 (14), 524 (13), 387 (12), 362 (12)	$C_{32}H_{46}O_8N_8$	336.17929	336.17921	0.25	SinAgm-2-7′/8-8′-DSinAgm [b]
21	13.80	326	$[M+H]^+$	337	306 (100), 320 (90), 206 (46), 321 (16), 114 (12), 303 (11)	$C_{16}H_{24}O_4N_4$	337.18716	337.18703	0.39	*trans*-SinAgm [b]
22	13.97	334	$[M+2H]^{2+}$	336	306 (100), 327 (24), 315 (13)	$C_{32}H_{46}O_8N_8$	336.17926	336.17921	0.16	SinAgm-8-8′/9-*N*-7′-DSinAgm [b]
23	21.82	366	$[M+2H]^{2+}$	306	276 (100), 297 (73), 455 (20), 285 (12), 289 (10)	$C_{30}H_{42}O_6N_8$	306.16870	306.16864	0.19	CouAgm-4-*O*-7′/3-8′-DSinAgm [e]
24	22.80	n.d.	$[M+2H]^{2+}$	306	276 (100), 297 (90), 455 (31), 265 (28), 285 (17), 228 (16), 481 (11), 456 (11)	$C_{30}H_{42}O_6N_8$	306.16861	306.16864	−0.11	CouAgm-4-*O*-7′/3-8′-DSinAgm [e]
25	10.78	342	$[M+2H]^{2+}$	321	291 (100), 256 (76), 300 (72), 131 (67), 361 (67), 312 (60), 511 (49), 157 (48), 328 (40), 370 (39), 344 (33), 327 (31), 242 (30), 114 (28), 226 (20), 181 (18), 483 (18), 624 (18), 494 (15)	$C_{31}H_{44}O_7N_8$	321.17404	321.17392	0.37	SinAgm-2-7′/8-8′-DFerAgm or FerAgm-2-7′/8-8′-DSinAgm [e]
26	12.54	n.d.	$[M+2H]^{2+}$	321	291 (100), 312 (22), 300 (15), 256 (10)	$C_{31}H_{44}O_7N_8$	321.17392	321.17392	−0.01	FerAgm-8-8′/9-*N*-7′-DSinAgm or SinAgm-8-8′/9-*N*-7′-DFerAgm [e]
27	15.37	n.d.	$[M+2H]^{2+}$	321	291 (100), 312 (27), 300 (11)	$C_{31}H_{44}O_7N_8$	321.17404	321.17392	0.37	FerAgm-8-8′/9-*N*-7′-DSinAgm or SinAgm-8-8′/9-*N*-7′-DFerAgm [e]
29	21.19	326	$[M+2H]^{2+}$	321	312 (100), 291 (99), 485 (59), 243 (37), 511 (19), 486 (17), 300 (17), 157 (15), 381 (11)	$C_{31}H_{44}O_7N_8$	321.17401	321.17392	0.27	FerAgm-4-*O*-7′/3-8′-DSinAgm [d,e](hordatine D)
31	23.06	326	$[M+2H]^{2+}$	321	291 (100), 312 (99), 485 (55), 243 (35), 511 (19), 486 (16), 300 (16), 157 (14), 381 (11)	$C_{31}H_{44}O_7N_8$	321.17395	321.17392	0.08	FerAgm-4-*O*-7′/3-8′-DSinAgm [d,e] (hordatine D)

[a] RP-UHPLC-PDA-IT-MS data of all peaks are shown in Supplementary data (Table S5).
[b] Compounds identified based on published fragmentation data (Van Zadelhoff, Meijvogel, et al., 2022).
[c,d] Compounds are stereoisomers.
[e] Compounds tentatively identified by matching fragmentation patterns (Supplementary data; Tables S1-S4).

performed the coupling of the combination of CouAgm and FerAgm at pH 5.3. Nonetheless, at this pH CouAgm was also only converted after all FerAgm had reacted and no CouAgm-FerAgm heterodimer formation was observed (data not shown).

3.6. Oxidative coupling by laccase

Although it was previously thought that a peroxidase is responsible for oxidative coupling of HCAgms in barley (Kristensen et al., 1999; Nomura et al., 2007), a recent study suggested that the oxidative coupling in barley is performed by a laccase (Ube et al., 2023). Moreover, it has been reported that hydroxycinnamic acid monomer reactivities were different when using different types of HRP and laccase (Takahama, 1995). Coupling of combinations of HCAgms by laccase has, however, not yet been studied. Unfortunately, laccase from barley is not commercially available, difficult to purify, and described to be unstable (Ube et al., 2023). Thus, to investigate whether the use of laccase rather than peroxidase would result in different reactivities or reaction products with combinations of HCAgms, the oxidative coupling was performed with two commercially available laccases (from *Agaricus bisporus* and *Trametes versicolor*). These incubations were performed in single-monomer systems, the combination of CouAgm and FerAgm, and a combination of all three monomers. Monomer conversion by both laccases was lower compared to the HRP incubation (Fig. 5), even though the enzyme dosage used for all incubations had the same enzyme activity based on the conversion of ABTS. Similar to the HRP incubations, CouAgm was always the least reactive monomer. For laccase from *Trametes versicolor*, the reactivity of FerAgm and SinAgm was the same. However, when all monomers were combined only SinAgm was converted for both laccases. SinAgm was the most reactive monomer in the three-compound combination, which aligns with the results previously reported for hydroxycinnamic acids (Takahama, 1995). All incubations with laccase resulted in the formation of the same products as in the incubations with HRP described here and in our previous work (Van Zadelhoff, Meijvogel, et al., 2022), indicating that the products formed are not enzyme-specific and that oxidative coupling of barley HCAgms could be performed by either a laccase or a peroxidase. Formation of the same product profile for HRP and laccase is in line with previous results for feruloyltyramine (Cardullo et al., 2016). An advantage of using a laccase rather than a peroxidase is that the use of H_2O_2 is not needed, which may make this a more suitable approach for industrial applications, for example. Similar to the incubation with HRP, upon incubation of a combination of CouAgm and FerAgm with laccase from *Trametes versicolor*, no CouAgm was converted. With laccase from *Agaricus bisporus* both monomers were converted into homodimers, but no heterodimers were detected either. Since the heterodimer of CouAgm and FerAgm is one of the most abundant neolignanamides in barley, these results indicate that the formation of this heterodimer might require the endogenous enzymes from barley or that an auxiliary factor besides peroxidase or laccase activity might be essential for the formation of this dimer. It has previously been shown that the formation of specific linkage types or stereoselective coupling products in plants depends on the presence of dirigent proteins, demonstrating involvement of dirigent proteins in the coupling process (Davin & Lewis, 2000; Davin et al., 1997; Kim & Sattely, 2021). In a previous study on the coupling of CouAgm using a dialysed barley seedling extract with peroxidase activity, the obtained dimers were present as a racemic mixture, whereas the natural dimers from barley are reported to be optically active (Negrel & Smith, 1984). This could suggest that dirigent proteins can also contribute to the formation of FerAgm and CouAgm heterodimers. On the other hand, one of these studies showed that the amount of heterodimers formed upon oxidative coupling did not change in the presence of dirigent proteins (Kim & Sattely, 2021). When using partly purified laccase from barley, Ube *et al.* produced optically active CouAgm dimers, although they could not exclude the involvement of dirigent proteins in their experiments (Ube et al., 2023). The potential involvement of dirigent proteins in the formation of (neo)lignanamides has not yet been investigated, but could explain how specific heterodimers, such as those of CouAgm and FerAgm, can be produced.

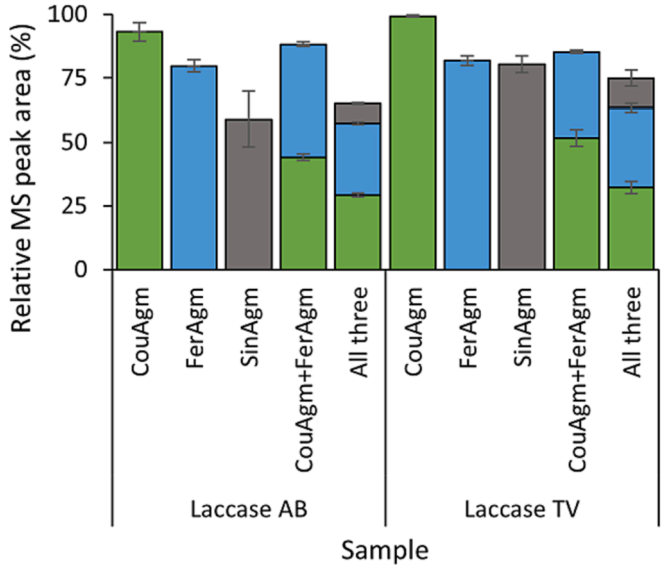

Fig. 5. Percentage of remaining monomer (t = 120 min) upon oxidative coupling of single compounds or combinations of coumaroylagmatine (CouAgm, green), feruloylagmatine (FerAgm, blue), and sinapoylagmatine (SinAgm, grey) with laccase from *Agaricus bisporus* (AB) or from *Trametes versicolor* (TV) expressed as the relative MS extracted ion peak area of the corresponding peak in RP-UHPLC-PDA-IT-MS. Error bars display the standard deviation based on triplicates. (For interpretation of the references to colour in this figure legend, the reader is referred to the web version of this article.)

3.7. Oligomerization upon oxidative coupling by HRP

Based on the formation of oligomers upon oxidative coupling in single-monomer systems (Van Zadelhoff, Meijvogel, et al., 2022) and the observed decrease in dimeric products after the 30 min time point of the oxidative coupling reaction in combined systems, the formation of oligomers was expected. The formation of oligomers was investigated using MALDI-TOF-MS. In all samples oligomers of degree of polymerization (DP) three and higher were formed (Supplementary data, Figure S4 and Table S6). In samples containing only FerAgm, the highest DP was 6 (Van Zadelhoff, Meijvogel, et al., 2022). This is in line with the DP that was observed for the CouAgm and FerAgm incubation, in which a FerAgm hexamer was detected. Since CouAgm conversion in this sample was very limited, the high DP is in line with the results for samples with only FerAgm.

The results presented in Fig. 2B indicate that the conversion of dimers to oligomers upon incubation of FerAgm and SinAgm is limited compared to the other incubations, which is reflected by the MALDI-TOF-MS data. It was observed that for the combinations of SinAgm with either CouAgm or FerAgm, no SinAgm homotrimers are formed and heterotrimers with two SinAgm and one CouAgm or FerAgm moiety were detected. The limited formation of larger SinAgm coupling

products, which was also previously observed in single-monomer systems (Van Zadelhoff, Meijvogel, et al., 2022), could be due to a restricted number of coupling options for SinAgm because of the presence of two methoxy groups on the aromatic ring. Furthermore, the most abundant linkage types formed for SinAgm, the 2-7′/8-8′-linkage and 8-8′/9-*N*-7′-linkage, are expected to limit the formation of larger coupling products as well, since most potential coupling positions are no longer available. For the combination of SinAgm and CouAgm, all trimers contain one CouAgm moiety, which is possibly due to CouAgm having more coupling options due to the absence of methoxy groups. The incorporation of CouAgm in larger coupling products could explain why CouAgm starts being converted before all SinAgm has been consumed, despite the much higher peak potential of CouAgm compared to SinAgm (Fig. 2A). No FerAgm and CouAgm heterodimers were detected by RP-UHPLC-PDA-IT-MS, however, with MALDI-TOF-MS a peak corresponding to the mass of this heterodimer was detected. Possibly, small amounts of various heterodimers with different linkage types were formed that were below limit of detection for RP-UHPLC-PDA-ITMS, but the total signal of all these heterodimers was high enough for detection by MALDI-TOF-MS. Dimeric and trimeric compounds with an additional OH-group were also detected. In previous work with HRP, the addition of an OH-group upon oxidative coupling was also observed. These compounds are by-products of the *in vitro* enzymatic oxidative coupling reaction and, based on their fragmentation pattern, have a different structure than the naturally occurring hydroxylated dimers (Van Zadelhoff, Meijvogel, et al., 2022).

4. Conclusion

In this work, we present *in vitro* oxidative coupling of combinations of hydroxycinnamoylagmatines (HCAgms) with HRP and H_2O_2 or laccase as a protocol for the production of sensory active and bioactive HCAgm homo- and heterodimers. In combinations of monomers, the order of reactivity of HCAgms remains the same as in single-monomer systems, with SinAgm being most reactive and CouAgm being least reactive. The products formed did not differ between incubations with HRP and H_2O_2 or the two tested laccases. The majority (>75 %) of dimeric coupling products are homodimers, with the 4-*O*-7′/3-8′-linkage as the main linkage type. Surprisingly, no heterodimers of CouAgm and FerAgm were detected, whereas heterodimers were detected for SinAgm with either CouAgm or FerAgm. As FerAgm-4-*O*-7′/3-8′-DCouAgm is commonly reported for barley, this indicates that the oxidative coupling of HCAgms in barley requires endogenous barley enzymes or involves more than just an oxidative enzyme. Overall, our results also provide insights into production of HCAgm dimers in more complex systems, such as in an *in vivo* environment. Furthermore, diagnostic fragments were identified for the differentiation of CouAgm-4-*O*-7′/3-8′-DFerAgm and FerAgm-4-*O*-7′/3-8′-DCouAgm, and of FerAgm-4-*O*-7′/3-8′-DFerAgm and CouAgm-4-*O*-7′/3-8′-DSinAgm. These diagnostic fragments also aid identification of these compounds in more complex systems, such as food matrices. In conclusion, our protocol for oxidative coupling combinations of hydroxycinnamoylagmatines yielded a set of structurally diverse homo- and heterodimers, facilitating production of these dimers for future studies on their sensory properties and bioactivity, and for establishing structure–property relationships.

Funding

This research received funding from the Netherlands Organisation for Scientific Research (NWO) by an NWO Graduate School Green Top Sectors grant (GSGT.2019.004).

CRediT authorship contribution statement

Annemiek van Zadelhoff: Writing – original draft, Visualization, Methodology, Investigation, Formal analysis, Conceptualization. **Jean-Paul Vincken:** Writing – review & editing, Supervision. **Wouter J.C. de Bruijn:** Writing – review & editing, Supervision, Methodology, Conceptualization.

Declaration of competing interest

The authors declare that they have no known competing financial interests or personal relationships that could have appeared to influence the work reported in this paper.

Data availability

Data will be made available on request.

Acknowledgements

Part of the presented results were obtained using a Thermo Scientific Velos Pro MS system and a Thermo Scientific Q Exactive Focus Orbitrap MS system, which are owned by Shared Research Facilities-WUR and subsidized by the province of Gelderland, The Netherlands.

Appendix A. Supplementary material

Supplementary data to this article can be found online at https://doi.org/10.1016/j.foodchem.2024.138898.

References

Akman, F. (2019). A density functional theory study based on monolignols: Molecular structure, homo-lumo analysis, molecular electrostatic potential. *Transport, 1*, 2.

Arrieta-Baez, D., & Stark, R. E. (2006). Modeling suberization with peroxidase-catalyzed polymerization of hydroxycinnamic acids: Cross-coupling and dimerization reactions. *Phytochemistry, 67*(7), 743–753. https://doi.org/10.1016/j.phytochem.2006.01.026

Arrieta-Baez, D., Dorantes-Álvarez, L., Martinez-Torres, R., Zepeda-Vallejo, G., Jaramillo-Flores, M. E., Ortiz-Moreno, A., & Aparicio-Ozores, G. (2012). Effect of thermal sterilization on ferulic, coumaric and cinnamic acids: Dimerization and antioxidant activity. *Journal of the Science of Food and Agriculture, 92*(13), 2715–2720. https://doi.org/10.1002/jsfa.5695

Baydoun, E.-A.-H., Pavlencheva, N., Cumming, C. M., Waldron, K. W., & Brett, C. T. (2004). Control of dehydrodiferulate cross-linking in pectins from sugar-beet tissues. *Phytochemistry, 65*(8), 1107–1115. https://doi.org/10.1016/j.phytochem.2004.02.014

Cardullo, N., Pulvirenti, L., Spatafora, C., Musso, N., Barresi, V., Condorelli, D. F., & Tringali, C. (2016). Dihydrobenzofuran neolignanamides: Laccase-mediated biomimetic synthesis and antiproliferative activity. *Journal of Natural Products, 79*(8), 2122–2134. https://doi.org/10.1021/acs.jnatprod.6b00577

Davin, L. B., & Lewis, N. G. (2000). Dirigent proteins and dirigent sites explain the mystery of specificity of radical precursor coupling in lignan and lignin biosynthesis. *Plant Physiology, 123*(2), 453–462. https://doi.org/10.1104/pp.123.2.453

Davin, L. B., Wang, H.-B., Crowell, A. L., Bedgar, D. L., Martin, D. M., Sarkanen, S., & Lewis, N. G. (1997). Stereoselective bimolecular phenoxy radical coupling by an auxiliary (dirigent) protein without an active center. *Science, 275*(5298), 362–367. https://doi.org/10.1126/science.275.5298.362

Elsler, B., Wiebe, A., Schollmeyer, D., Dyballa, K. M., Franke, R., & Waldvogel, S. R. (2015). Source of selectivity in oxidative cross-coupling of aryls by solvent effect of 1,1,1,3,3,3-hexafluoropropan-2-ol. *Chemistry–A European Journal, 21*(35), 12321–12325. https://doi.org/10.1002/chem.201501604

Gaspar, A., Garrido, E. M., Esteves, M., Quezada, E., Milhazes, N., Garrido, J., & Borges, F. (2009). New insights into the antioxidant activity of hydroxycinnamic acids: Synthesis and physicochemical characterization of novel halogenated derivatives. *European Journal of Medicinal Chemistry, 44*(5), 2092–2099. https://doi.org/10.1016/j.ejmech.2008.10.027

Gorzolka, K., Bednarz, H., & Niehaus, K. (2014). Detection and localization of novel hordatine-like compounds and glycosylated derivates of hordatines by imaging mass spectrometry of barley seeds. *Planta, 239*(6), 1321–1335. https://doi.org/10.1007/s00425-014-2061-y

Heuberger, A. L., Broeckling, C. D., Lewis, M. R., Salazar, L., Bouckaert, P., & Prenni, J. E. (2012). Metabolomic profiling of beer reveals effect of temperature on non-volatile small molecules during short-term storage. *Food Chemistry, 135*(3), 1284–1289. https://doi.org/10.1016/j.foodchem.2012.05.048

Kageyama, N., Inui, T., Fukami, H., & Komura, H. (2011). Elucidation of chemical structures of components responsible for beer aftertaste. *Journal of the American Society of Brewing Chemists, 69*(4), 255–259. https://doi.org/10.1094/ASBCJ-2011-0901-01

Kageyama, N., Inui, T., Nakahara, K., & Fukami, H. (2013). Beer aftertaste improved by reducing astringent substances in the barley malt with subcritical water treatment.

Journal of the American Society of Brewing Chemists, 71(3), 105–108. https://doi.org/10.1094/ASBCJ-2013-0422-01

Kim, S. S., & Sattely, E. S. (2021). Dirigent proteins guide asymmetric heterocoupling for the synthesis of complex natural product analogues. *Journal of the American Chemical Society, 143*(13), 5011–5021. https://doi.org/10.1021/jacs.0c13164

Kočovský, P., Vyskočil, S., & Smrcina, M. (2003). Non-symmetrically substituted 1,1'-binaphthyls in enantioselective catalysis. *Chemical Reviews, 103*(8), 3213–3246. https://doi.org/10.1021/cr9900230

Koistinen, V. M., Tuomainen, M., Lehtinen, P., Peltola, P., Auriola, S., Jonsson, K., & Hanhineva, K. (2020). Side-stream products of malting: A neglected source of phytochemicals. *npj Science of Food, 4*(1), 21. https://doi.org/10.1038/s41538-020-00081-0

Kristensen, B. K., Bloch, H., & Rasmussen, S. K. (1999). Barley coleoptile peroxidases. Purification, molecular cloning, and induction by pathogens. *Plant Physiology, 120*(2), 501–512. https://doi.org/10.1104/pp.120.2.501

Kristensen, B. K., Burhenne, K., & Rasmussen, S. K. (2004). Peroxidases and the metabolism of hydroxycinnamic acid amides in *Poaceae*. *Phytochemistry Reviews, 3*(1–2), 127–140. https://doi.org/10.1023/B:PHYT.0000047800.59980.6e

Kulichikhin, K. Y., Aitio, O., Chirkova, T. V., & Fagerstedt, K. V. (2007). Effect of oxygen concentration on intracellular ph, glucose-6-phosphate and ntp content in rice (*Oryza sativa*) and wheat (*Triticum aestivum*) root tips: In vivo 31p-NMR study. *Physiologia Plantarum, 129*(3), 507–518. https://doi.org/10.1111/j.1399-3054.2006.00819.x

Lafontaine, S., Senn, K., Knoke, L., Schubert, C., Dennenlöhr, J., Maxminer, J., … Heymann, H. (2020). Evaluating the chemical components and flavor characteristics responsible for triggering the perception of "beer flavor" in non-alcoholic beer. *Foods, 9*(12), 1914. https://doi.org/10.3390/foods9121914

Leifert, D., & Studer, A. (2020). The persistent radical effect in organic synthesis. *Angewandte Chemie International Edition, 59*(1), 74–108. https://doi.org/10.1002/anie.201903726

Leonard, W., Zhang, P., Ying, D., & Fang, Z. (2020). Lignanamides: Sources, biosynthesis and potential health benefits–a minireview. *Critical Reviews in Food Science and Nutrition, 1–11*. https://doi.org/10.1080/10408398.2020.1759025

Libman, A., Shalit, H., Vainer, Y., Narute, S., Kozuch, S., & Pappo, D. (2015). Synthetic and predictive approach to unsymmetrical biphenols by iron-catalyzed chelated radical–anion oxidative coupling. *Journal of the American Chemical Society, 137*(35), 11453–11460. https://doi.org/10.1021/jacs.5b06494

Magoulas, G. E., & Papaioannou, D. (2014). Bioinspired syntheses of dimeric hydroxycinnamic acids (lignans) and hybrids, using phenol oxidative coupling as key reaction, and medicinal significance thereof. *Molecules, 19*(12), 19769–19835. https://doi.org/10.3390/molecules191219769

Mikkelsen, B., Olsen, C., & Lyngkjær, M. (2015). Accumulation of secondary metabolites in healthy and diseased barley, grown under future climate levels of CO^2, ozone and temperature. *Phytochemistry, 118*, 162–173. https://doi.org/10.1016/j.phytochem.2015.07.007

Negrel, J., & Smith, T. A. (1984). Oxidation of *p*-coumaroylagmatine in barley seedling extracts in the presence of hydrogen peroxide or thiols. *Phytochemistry, 23*(4), 739–741. https://doi.org/10.1016/S0031-9422(00)85015-3

Neudörffer, A., Bonnefont-Rousselot, D., Legrand, A., Fleury, M.-B., & Largeron, M. (2004). 4-hydroxycinnamic ethyl ester derivatives and related dehydrodimers: Relationship between oxidation potential and protective effects against oxidation of low-density lipoproteins. *Journal of Agricultural and Food Chemistry, 52*(7), 2084–2091. https://doi.org/10.1021/jf035068n

Nomura, T., Ishizuka, A., Kishida, K., Islam, A. K., Endo, T. R., Iwamura, H., & Ishihara, A. (2007). Chromosome arm location of the genes for the biosynthesis of hordatines in barley. *Genes & Genetic Systems, 82*(6), 455–464. https://doi.org/10.1266/ggs.82.455

Okazaki, Y., Ishihara, A., Nishioka, T., & Iwamura, H. (2004). Identification of a dehydrodimer of avenanthramide phytoalexin in oats. *Tetrahedron, 60*(22), 4765–4771. https://doi.org/10.1016/j.tet.2004.04.008

Okazaki, Y., Ishizuka, A., Ishihara, A., Nishioka, T., & Iwamura, H. (2007). New dimeric compounds of avenanthramide phytoalexin in oats. *The Journal of Organic Chemistry, 72*(10), 3830–3839. https://doi.org/10.1021/jo0701740

Oladokun, O., Tarrega, A., James, S., Smart, K., Hort, J., & Cook, D. (2016). The impact of hop bitter acid and polyphenol profiles on the perceived bitterness of beer. *Food Chemistry, 205*, 212–220. https://doi.org/10.1016/j.foodchem.2016.03.023

Pihlava, J.-M. (2014). Identification of hordatines and other phenolamides in barley (*Hordeum vulgare*) and beer by UPLC-QTOF-MS. *Journal of Cereal Science, 60*(3), 645–652. https://doi.org/10.1016/j.jcs.2014.07.002

Pihlava, J. M., Kurtelius, T., & Hurme, T. (2016). Total hordatine content in different types of beers. *Journal of the Institute of Brewing, 122*(2), 212–217. https://doi.org/10.1002/jib.311

Schön, F., Kaifer, E., & Himmel, H. J. (2019). Catalytic aerobic phenol homo-and cross-coupling reactions with copper complexes bearing redox-active guanidine ligands. *Chemistry–A European Journal, 25*(35), 8279–8288. https://doi.org/10.1002/chem.201900583

Smith, T. A., & Best, G. R. (1978). Distribution of the hordatines in barley. *Phytochemistry, 17*(7), 1093–1098. https://doi.org/10.1016/S0031-9422(00)94295-X

Stoessl, A. (1967). The antifungal factors in barley. IV. Isolation, structure, and synthesis of the hordatines. *Canadian Journal of Chemistry, 45*(15), 1745–1760. https://doi.org/10.1139/v67-283

Stoessl, A., & Unwin, C. (1970). The antifungal factors in barley. V. Antifungal activity of the hordatines. *Canadian Journal of Botany, 48*(3), 465–470. https://doi.org/10.1139/b70-066

Syrjänen, K., & Brunow, G. (1998). Oxidative cross coupling of *p*-hydroxycinnamic alcohols with dimeric arylglycerol β-aryl ether lignin model compounds. The effect of oxidation potentials. *Journal of the Chemical Society, Perkin Transactions, 1*(20), 3425–3430. https://doi.org/10.1039/A805349I

Takahama, U. (1995). Oxidation of hydroxycinnamic acid and hydroxycinnamyl alcohol derivatives by laccase and peroxidase. Interactions among *p*-hydroxyphenyl, guaiacyl and syringyl groups during the oxidation reactions. *Physiologia Plantarum, 93*(1), 61–68. https://doi.org/10.1034/j.1399-3054.1995.930110.x

Ube, N., Ishihara, A., Yabuta, Y., Taketa, S., Kato, Y., & Nomura, T. (2023). Molecular identification of a laccase that catalyzes the oxidative coupling of a hydroxycinnamic acid amide for hordatine biosynthesis in barley. *The Plant Journal, 115*(4), 1037–1050. https://doi.org/10.1111/tpj.16278

Ube, N., Nishizaka, M., Ichiyanagi, T., Ueno, K., Taketa, S., & Ishihara, A. (2017). Evolutionary changes in defensive specialized metabolism in the genus *Hordeum*. *Phytochemistry, 141*, 1–10. https://doi.org/10.1016/j.phytochem.2017.05.004

van Zadelhoff, A., de Bruijn, W. J. C., Fang, Z., Gaquerel, E., Ishihara, A., Werck-Reichhart, D.l., … Vincken, J. P. (2021). Toward a systematic nomenclature for (neo)lignanamides. *Journal of Natural Products, 84*(4), 956–963. https://doi.org/10.1021/acs.jnatprod.0c00792

Van Zadelhoff, A., Meijvogel, L., Seelen, A.-M., de Bruijn, W. J. C., & Vincken, J.-P. (2022). Biomimetic enzymatic oxidative coupling of barley phenolamides: Hydroxycinnamoylagmatines. *Journal of Agricultural and Food Chemistry, 70*(51), 16241–16252. https://doi.org/10.1021/acs.jafc.2c07457

van Zadelhoff, A., Vincken, J.-P., & de Bruijn, W. J. C. (2022). Facile amidation of non-protected hydroxycinnamic acids for the synthesis of natural phenol amides. *Molecules, 27*(7), 2203. https://doi.org/10.3390/molecules27072203

Wakimoto, T., Nitta, M., Kasahara, K., Chiba, T., Yiping, Y., Tsuji, K., … Koike, M. (2009). Structure–activity relationship study on α1 adrenergic receptor antagonists from beer. *Bioorganic and Medicinal Chemistry Letters, 19*(20), 5905–5908. https://doi.org/10.1016/j.bmcl.2009.08.068

Zipor, G., & Oren-Shamir, M. (2013). Do vacuolar peroxidases act as plant caretakers? *Plant Science, 199*, 41–47. https://doi.org/10.1016/j.plantsci.2012.09.018